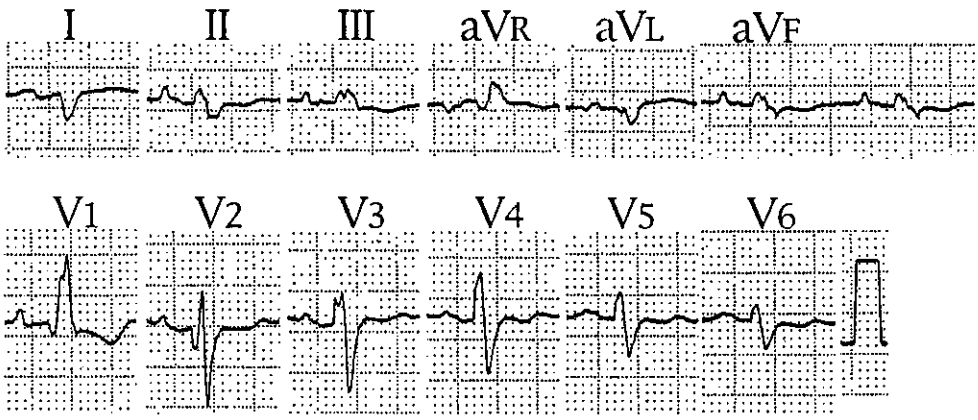

Fig. 1 The electrocardiogram has apositive P wave in lead II, and shows a normal sinus rhythm at the rate 60 beats per minute. Although the amplitude of P wave in leads II and III was not high enough to meet the criteria for right atrial overload, peaking of the first half of the P wave in lead VI may be a reflection of the overload of the right atrium. The PQ interval was within the normal range. The right axis deviation and clockwise rotation of the QRS complex may be due to right ventricular overload. The width of the QRS complex was 168 msec, and the rS pattern in V6 with a wide S wave suggests complete right bundle branch block (CRBBB); however, the QRS complex in V1 was not an typical CRBBB rsR pattern. There was an abnormal Q wave in V1 and V2, which raises the possibility of myocardial necrosis in the ventricular septum. Slight ST depression and biphasic T wave are seen in the left precordial leads.

Dr. Matsumura: The right jugular vein was found to be distended up to the level of the mandible, and *a* v wave was observed.

Dr. Ogawa: The marked distension of the jugular vein indicates that the filling pressure of the right cardiac system was high, doesn't it? The respiratory rate was also increased. How about the cardiac murmur?

Dr. Matsumura: The murmur was pansystolic. Echocardiography suggested the presence of mitral regurgitation (MR) and tricuspid regurgitation (TR), and the murmur was considered to be associated with these regurgitations.

Dr. Ogawa: Do you mean that the signs of right heart failure were rather significant?

Dr. Matsumura: Yes, that's right.

Dr. Ogawa: Will you please present the results of arterial blood gas analysis?

Dr. Matsumura: Under nasal administaration of 2 L/Min oxygen, the pH was 7.44; Pco_2, 31.4 Torr; Po_2, 144.4 Torr; HCO_3^-, 24.5 mEq/L; BE 1.5, mEq/L; and the Sao_2, 99.4%. These findings are suggestive of compensated respiratory alkalosis from hyperventilation.

Dr. Ogawa: How can we correlate the findings of the morbid condition reported in this conference with the ECG findings? What is your opinion, Dr. Mitamura? (Fig. 1)

Dr. Mitamura: The ECG fundamentally revealed a sinus rhythm. An occasional ventricular extrasystole was observed in the limb leads.

As to the P wave, the negative portion of P wave in lead V1 did not seem to be so clear. There seemed to be some peaking of the first half of the P wave, suggestive of right atrial overload.

The PQ interval was almost within the normal range. The QRS axis deviated to the right, and as stated earlier, the right axis deviation may be reflective of right ventricular overload. However, the axis might be influenced by a right bundle branch block. The first component in leads V1 and V2 in cases of right bundle branch block is essentially an upright r, but in this case there was a negative deflection, a "q" wave, in these leads. This matter weighs on my mind. The presence of the "q" wave in these two leads may suggest the possibility of myocardial necrosis in the ventricular septum. Mild non specific ST-T changes were observed in the chest leads.

The patient had a thoracic deformity, and there is the possibility that this also influenced the ECG changes. It would therefore seem difficult to make a definitive diagnosis based on the ECG findings alone in this patient.

Dr. Ogawa: The presence of abnormal "q" waves in leads V1 and V2 in a case with right bundle branch block should raise the possibility of cardiac sarcoidosis, which selectively damages the interventricular septum.

Dr. Matsumura: A chest X-ray taken in the year 2000, when the patient was being followed up as an outpatient, is shown here. There is thoracic deformity and collapse of the right lung, which are probably consequent to the traffic accident. The mediastinum is shifted to the left. There is no obvious evidence of pulmonary venous congestion, such as the presence of Kerley's B lines. There is no evidence of pulmonary venous re-distribution to the upper lung fields. The tracheal bifurcation angle is approximately 90°, which suggests the presence of left atrial dilatation.

In the lateral view, narrowing of the retrosternal space is observed, which suggests the presence of right

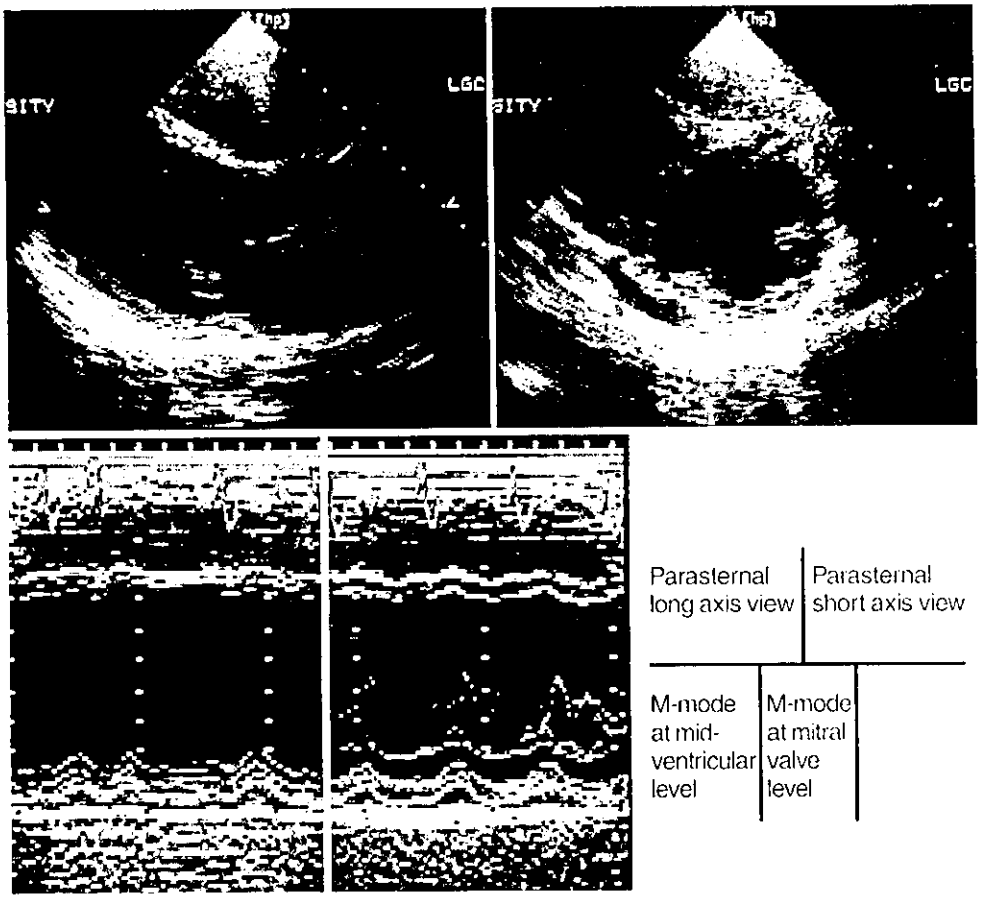

Fig. 2 The echocardiography was performed on March 28, 2001. Parasternal long axis view on the left upper panel shows dilation of the left and right ventricles. Thinning of the left ventricular wall and a small amount of pericardial effusion are also observed on the right upper panel, the parasternal short axis view. The two lower panels are M-mode traces at the mid-ventricular level (left) and mitral valve (right). Both traces revealed reduced excursion and thinning of the left ventricular wall. The calculated ejection fraction of the left ventricle was 23% by the method of Pombo, suggesting marked reduction of left ventricular systolic function. B-B′ step of mitral valve on the right lower panel suggests the elevation of left ventricular end-diastolic pressure.

ventricular dilatation. Dilatation of the left ventricle is also suspected from the point of intersection between the diaphragm and the inferior vena cava. The costophrenic angles are sharp, and there is no evidence of pleural effusion.

This X-ray taken on admission to our hospital shows opacity of the right lung field. The cardiothoracic ratio (CTR) is slightly high, and no Kerley's B lines are evident. These findings suggest that there was no significant pulmonary venous congestion. There is no evidence of pleural effusion. There is also evidence suggestive of dilatation of the left atrium and right ventricle.

Dr. Ogawa: The left ventricular function was significantly compromised in this patient, but findings of right heart failure were more remarkable on admission. There was no evidence of pulmonary congestion, either clinically or on chest X-ray. Will you present the echocardiographic findings in this patient and explain his heart condition as evaluated by this investigation, Dr. Iwanaga? (Fig. 2)

Dr. Iwanaga (Laboratory Medicine): This videotape shows the echocardiographic findings of this patient obtained on March 28. The parasternal long-axis view shows the right and left ventricles, left atrium, aorta, mitral valve, and the aortic valve. The short-axis view shows the right atrium and right ventricle. We can see a Swan-Ganz catheter inserted. At the level of the papillary muscle, the interventricular septum is slightly hyperechoic, which shows little or no wall motion. The motion of the posterior wall is also poor, and the left ventricle is dilated. As for the valves, moderate to severe MR is observed. The aortic valve shows atherosclerotic degeneration. The most significant findings are the dilated left ventricle and the poor contraction of the interventricular septum and posterior wall. The mitral regurgitation may be due to dilatation of the left ventricle and the mitral annulus. The left ventricular

diameter as measured by M-mode was 6 cm and 5.5 cm at end-diastole and end-systole, respectively, which reflects significant dilatation. A small amount of pericardial effusion is also observed.

The apical four-chamber view shows that the contraction of the interventricular septum is even worse than that of the free wall, even though there is significant thinning of the free wall. The left atrium is dilated. Wall motion of the free wall is relatively sustained, but, on the whole, left ventricular contractile dysfunction is diffuse. Based on these echocardiographic findings, the diagnosis of DCM is suspected. One problem, however, is localization of the wall thinning; the thinning is distributed in the areas supplied by the right coronary and left anterior descending arteries. Marked fibrosis is evident in these areas. It is impossible to completely rule out left ventricular contractile dysfunction due to ischemic heart disease from this finding.

Dr. Ogawa: What do you think of the possibility of cardiac sarcoidosis in this case?

Dr. Iwanaga: In cardiac sarcoidosis, a relatively localized contractile dysfunction of the left ventricle is observed, and wall motion remains relatively normal in other areas. Reports of diffuse hypokinesis of the left ventricle, as observed in the present case, are limited. A color Doppler image of the apical four chamber view is shown. Severe TR is evident from this image.

Dr. Ogawa: Is there any evidence of an organic legion in the tricuspid valve?

Dr. Iwanaga: The TR could be related to the presence of the Swan-Ganz catheter through the tricuspid valve and annular dilatation consequent to dilatation of the right ventricle. The patient had only mild pulmonary hypertension; the pulmonary arterial pressure was estimated to be 31/21 mmHg. This is reflective of postcapillary pulmonary hypertension due to left heart failure.

From the echocardiographic findings, DCM may be suspected as the first differential diagnosis, and in the present case, it was presumably severe and associated with hemodynamic decompensation. However, in the presence of thinning of the ventricular wall in the areas of the right coronary artery and left anterior descending artery, it is difficult to rule out so-called ischemic cardiomyopathy.

Dr. Ogawa: When DCM is suspected, primary DCM should be differentiated from secondary DCM. The ischemic DCM just mentioned by Dr. Iwanaga cannot be ruled out, either. While cardiac sarcoidosis may be kept in mind, the possibility is rather remote, because in this case, not only the interventricular septum, in which lesions usually develop, but also the free wall of the left ventricular myocardium, showed significant diffuse damage. The presence of a positive family history also points more towards the possibility of primary or hereditary DCM.

Now, Dr. Matsumura, could you please outline the treatment initiated in this case?

Dr. Matsumura: In 1993, when the patient was first admitted to our hospital, treatment with digitalis, Warfarin®, an ACE inhibitor, and furosemide was started. Thereafter, the patient was followed up on outpatient basis. Sometime in mid 1997, the patient was readmitted with symptoms of a common cold and worsening of his heart failure. On that occasion, administration of a β-blocker was initiated, and when the patient showed improvement, he was discharged. However, with the continuation of the β-blocker, the symptoms of heart failure, including leg edema and dyspnea on exertion (DOE), gradually became worse, and administration of the β-blocker was discontinued.

Subsequently, when the patient was admitted once again with worsening of heart failure, administration of Acardi® (pimobendan), a phosphodiesterase (PDE) inhibitor that also enhances the calcium sensitivity of myocardial cells, was initiated. In addition, the dose of the diuretic was increased and spironolactone was started. The subsequent course of the patient was again monitored on outpatient basis.

Dr. Ogawa: Do you have any comments about the course of treatment undertaken so far, Dr. Yoshikawa?

Dr. Yoshikawa (Internal Medicine): The standard treatment for all cases ranging from asymptomatic left ventricular dysfunction to severe heart failure includes administration of ACE inhibitors or angiotensin type I receptor antagonists. For mild to moderate heart failure classified as NYHA functional class II or III, diuretics are usually added to the treatment regimen, and in some patients, also digitalis. Some reports have shown that the prognosis is improved by the administration of a β-blocker in such patients. Furthermore, in severe heart failure classified as NYHA functional class III or IV, further improvement of prognosis has been reported with the addition of spironolactone to the treatment regimen. Although pimobendan does not decrease the mortality rate, clinical studies in Japan have shown that the drug decreases the number of patients who are admitted to hospitals due to worsening heart failure, *i.e.*, it improves the quality of life. With regard to Warfarin®, there is limited evidence to suggest improvement in the prognosis of these patients, as there have been no large-scale studies on the treatment of heart failure with this drug.

Dr. Ogawa: How about digitalis?

Dr. Yoshikawa: Some data have shown that digitalis significantly decreases the mortality associated with worsening heart failure. The overall mortality, however, has been reported to be similar between groups receiving digitalis and placebo. The reason for this is unclear, but digitalis probably increases the incidence

of sudden death. Accordingly, there has been a gradual tendency towards reduced usage of this drug.

Dr. Ogawa: Dr. Matsumura, could you please describe the course of this patient after admission?

Dr. Matsumura: The blood pressure on admission was 118/75 mmHg, and frequent non sustained ventricular tachycardia were observed. With a Swan-Ganz catheter, the pulmonary arterial pressure was determined to be 43/33 mmHg; the right atrial pressure, 19 mmHg; the cardiac index, 1.1 L/min/m^2 BSA; and the cardiac output, 1.8 L/min. Thus, all of these values were abnormal, and the pulmonary arterial oxygen saturation was markedly decreased to 33%. Intravenous injections of furosemide and continuous infusion of dobutamine, which had been initiated for the treatment of heart failure at the Nihon University Hospital, were continued. Administration of amiodarone for the treatment of ventricular tachycardia, and also of Adehl®, (colforsin daropate hydrochloride) as an inotropic agent, was started. The hemodynamic status improved slightly, the cardiac index and right atrial pressure improving to 1.4 and 16, respectively, however, oliguria and gradual deterioration of renal function were observed.

On March 9, elevation of the BUN/Cr and K levels to 93.5/6.0 and 6.0, respectively, were observed, and continuous hemodiafiltration (CHDF) was initiated. With the start of CHDF, the serum Cr and K levels decreased gradually to 2.7 and 3.9, respectively, while the heart rate started increasing.

With stabilization of the serum Cr and K levels, CHDF was temporarily discontinued on March 27. However, the patient could not be indefinitely sustained without CHDF, and the procedure was started again on March 31. Wide QRS tachycardia began to be observed on this day, and severe hepatic dysfunction was noted on April 3. Hemodialysis (HD) was started to wean the patient from CHDF, performed once every two days, and the course of the patient was carefully monitored. The wide QRS tachycardia and severe hepatic dysfunction improved slightly, but the patient's general condition continued to deteriorate. On April 14, elevation of the central venous pressure, deterioration of renal function, and decreased consciousness level were observed, and CHDF was started again.

The consciousness disturbance deteriorated on April 15. On April 17, in deference to the family's wishes, CHDF was discontinued. On the evening of the 18th, the patient started gasping, and developed respiratory arrest at 18:20 p.m. Thereafter, cardiac arrest occurred at 18:30 p.m., and the patient was declared dead.

Dr. Ogawa: The patient, who had DCM, was referred to our hospital with consciousness disturbance. He had severe cardiac dysfunction. How should the data collected with the Swan-Ganz catheter be interpreted?

Dr. Matsumura: According to Forrester's classification of hemodynamic disturbance in acute myocardial infarction, heart failure is classified as group IV. In this category of patients, not only diuretics, but also an inotropic agents are considered to be indicated.

Dr. Ogawa: Could you please explain the changes in the ANP and BNP data in relation to the severity of the heart failure?

Dr. Matsumura: The serum level of BNP was 2,356 in 1997, which decreased in subsequent examinations to 1,557 and 1,217. The level of ANP was 100 to 700, showing no remarkable changes thereafter. On admission, the BNP level was significantly elevated to 5,410, consistent with deterioration of the heart failure. BNP, which is a protein discovered from swine brain, is reported to be secreted mainly from the ventricular cardiomyocytes in humans. The normal serum BNP level is 15 or less, and the levels are elevated in heart failure. Our patient showed markedly elevated levels of BNP.

Dr. Ogawa: Initially, I thought that the present admission may have been directly related to the ventricular arrhythmia. However, judging from the course, the cardiac failure also seems to have worsened considerably, and there is the possibility that the nonsustained ventricular tachycardia was related to the worsening of the cardiac function. Am I right?

Dr. Matsumura: Yes, Sir.

Dr. Ogawa: What about other possibilities for the ventricular tachycardia, such as its being a possible proarrhythmic effect of one of the drugs used?

Dr. Matsumura: The possibility of pimobendan, an inotropic agent, having triggered the ventricular tachycardia cannot be ruled out.

Dr. Ogawa: What was the blood level of digoxin?

Dr. Matsumura: It was slightly elevated to 2.2. The echocardiographic findings showed that the size of the left ventricle was almost unchanged, but the short-axis view revealed deterioration of wall motion and thinning of the wall. These observations suggest the possibility that the frequent runs of ventricular tachycardia were triggered by increasing severity of the cardiomyopathy itself.

Dr. Ogawa: Cardiomyopathy itself in this case had progressed considerably, and such progression secondarily induced frequent episodes of tachycardia. This also may have contributed to the worsening of the morbid condition of the patient.

As a last issue regarding the clinical course of the patient, the serum Cr level in the patient on admission was 2.6. Thereafter, the renal function deteriorated rapidly, necessitating the introduction of hemodialysis (HD). I would like to now ask Dr. Kumagai to explain the patient's overall pathological findings in relation to the changes in the renal function and CHDF.

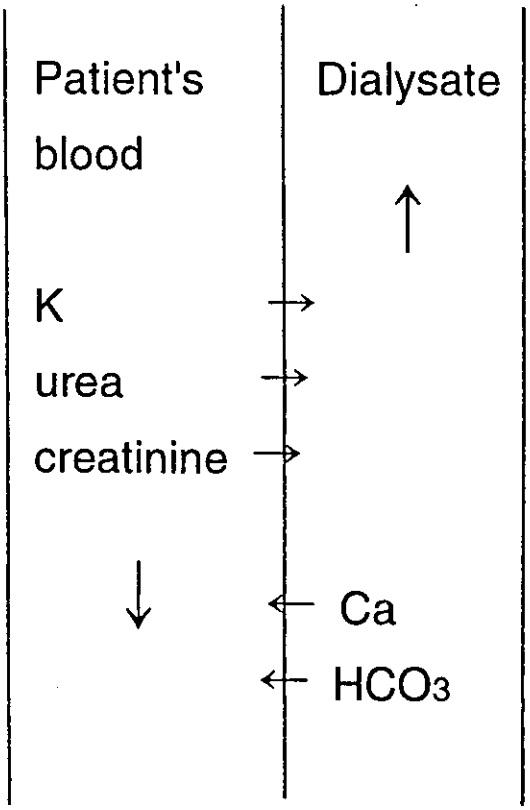

Fig. 3 The principle underlying the commonly performed hemodialysis (HD).

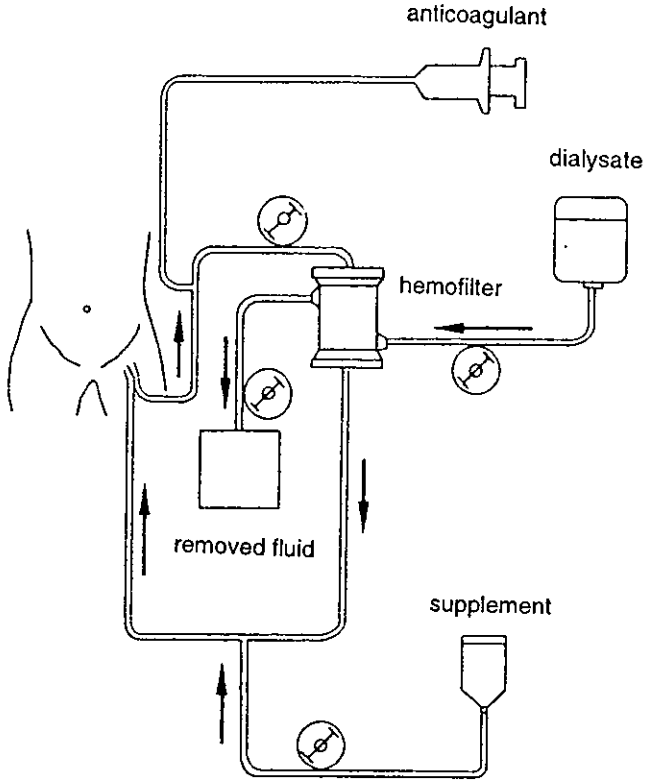

Fig. 4 A schema of continuous hemodiafiltration (CHDF). As in the commonly performed HD, the HD solution and the patient's blood are allowed to flow in reverse directions and to come in contact with each other; then a supplementary solution is added to the blood.

Dr. Kumagai (Internal Medicine): On admission, serum Cr level of the patient was 2.6 mg/dl and BUN level was approximately 60 ml/dl, but thereafter, the renal function deteriorated gradually. The deterioration can be explained by following mechanism: renal blood flow (RBF) is one-fourth of normal cardiac output despite their small size; it is well known that the RBF becomes extremely reduced in a situation of low cardiac output.

The BUN to Cr ratio is usually somewhere between 10:1 and 20:1. Thus given for a serum Cr level of 2.6, the corresponding BUN level should have been 30 to 40, whereas it was actually 60 in this patient. To explain this discrepancy, it is important to consider this patient's use of a diuretic (furosemide, Lasix®). Diuretics cause dehydration and vasopressin release, which makes water reabsorption at the collecting ducts of the kidneys. Vasopressin causes the reabsorption of urea from the tubules. On the other hand, Cr is filtered only at the glomeruli and is not reabsorbed in the renal tubules. Therefore, even though vasopressin is released, blood level of Cr does not increase. Since only urea is reabsorbed, the urea nitrogen level is relatively increased as compared with serum Cr level when a diuretic is used for the resolution of pulmonary congestion and in the presence of dehydration.

Although the cardiac function improved somewhat due to the use of furosemide, the cardiac index still did not reach 2, and the patient's renal function continued to deteriorate, and eventually CHDF became necessary.

In the conventional hemodialysis (HD) shown Fig. 3, the patient's blood and HD solution are allowed to flow as counter currents, and the excess K, urea, Cr, and water in the patient's blood are removed from the patient's blood into the HD solution. Conversely, substances that are beneficial for the patient (calcium, bicarbonate ion), which are contained in the HD solution, enter the patient's blood.

In CHDF, shown in Fig. 4, the mechanism is basically the same as in HD, but since it is a continuous system, the load on the patient's cardiovascular system is comparatively lighter. HD is impossible in the presence of a low cardiac output associated with hypotension, as in this patient. That is the reason why we chose the CHDF for this patient.

The two merits of CHDF are shown in Table 2. (1) the load on the cardiovascular system is lighter as compared to that during HD and hypotension is less common in CHDF. In the healthy humans, approximately 3

Table 2 Merits and Significance of CHDF

1. It imposes only a slight load on the cardiovascular system and scarcely causes a decrease in blood pressure.
   HD: 3 L of fluid is forced to be removed (volume normally removed over 2 days) in 4 hours. Electrolytes, such as Na, K are rapidly eliminated. Even though the molecular weight of these substances is low, a unit of osmotic pressure is decreased by elimination of one molecule. Consequently, with the decrease in the osmotic pressure, the blood pressure may decrease. This potential decline is not compensated for in HD.
   Normal kidneys: A volume of 3 L is removed in 2 days.
   CHDF: The volume of 3 L can be removed in 2 days. When one molecule is eliminated, the a unit of osmotic pressure is decreased; however, this decrease is compensated for in CHDF.
2. Substances with molecular weights of 1,000–15,000, which cannot be eliminated by HD, can be eliminated by CHDF.

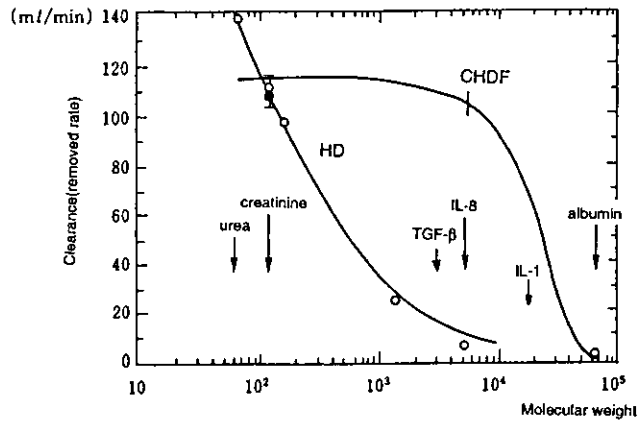

Fig. 5 Relationships between the molecular weights of substances eliminated by HD and CHDF and the elimination rates (clearance). Substances with molecular weights of 1,000 to 10,000 (e.g., TGFβ and IL-8) show a high clearance with CHDF.

L of urine are excreted from the capillaries of the renal glomeruli in 2 days. The same excretion can be obtained by CHDF. In contrast, in HD, 3 L of water are removed within 4 hours. (2) CHDF can remove substances with molecular weights between 1,000 and 15,000, which cannot be removed by HD. Cytokines and some growth factors are involved in the development of heart failure. As shown Fig. 5, the curve running steeply from the upper left side to the lower right side illustrates how substances are removed during HD, and the less steep curve alongside it on the right illustrates how substances are removed during CHDF. The molecular weights of the substances are plotted along the horizontal axis, and the volume (clearance) of the substances removed from the patient's blood is plotted along the longitudinal axis. Substances, such as urea, Cr and uric acid, of which molecular weights are 100 to 1,000, are removed efficiently by HD.

However, the substances of which molecular weights are 1,000 to 10,000 or 15,000, such as TGF-β, IL-8, and IL-1, cannot be removed by HD and can be by CHDF. Since these substances may be involved in the exacerbation of heart failure, removal of these substances by CHDF is desirable.

On the other hand, CHDF has some demerits; patients are connected to devices with tubes all day long, because it is a continuous process. This is a big disadvantage for patients. Usually, the procedure is performed over 24 hours a day for about 3 days, and when a significant improvement is observed, it is discontinued for the subsequent 2 days. CHDF can also be switched to the conventional HD (conducted for 4–5 hours every other day or every day). In the present patient, however, CHDF was successful; since the cardiac index increased slightly, and the pulmonary arterial wedge pressure decreased. The physician-in-charge wanted for CHDF to be continued. Throughout the treatment, the highly intelligent patient was conscious and alert. He and his wife hoped that the CHDF be continued for longer. Under these circumstances, CHDF was continued for subsequent 20 days, with only a few interruptions, although such long-term continuation of this procedure is quite exceptional.

Since the patient is connected to tubes and devices and the anticoagulant (heparin) is used during CHDF, the risk of hemorrhage should be always borne in mind. Therefore, the patient's condition has to be closely monitored. It is usually difficult to continue CHDF for a long term, but it was continued in this patient because he was extremely cooperative.

Dr. Ogawa: Heart failure is always associated with various degrees of renal dysfunction. While this new treatment was temporarily efficient, it could not influence the deterioration in cardiac function or improve the low cardiac output.

Dr. Sato, could you please comment on assisted circulation as a possible method of treatment, and also other novel methods of treatment for heart failure?

Dr. Satoh (Internal Medicine): We had administered almost all the drugs available for the treatment of heart failure, including CHDF. We had planned to make the patient register for a heart transplantation and wait for donors when his condition had improved a little more.

Dr. Ogawa: As for registration for heart transplantation, would this patient have met the criteria for such registration? What are the current criteria for registration?

Dr. Yoshikawa: There are various criteria: *e.g.*, it is recommended that the patient be younger than 60 years old, that the patient be on a β-blocker, that the pulmonary vascular resistance be less than 6 wood unit, and that there be no serious infectious diseases, such as human immunodeficiency virus infection.

Anyway, our patient had severe heart failure, with a serum BNP level of 5,000 pg/mL, and he would have been a good candidate for heart transplantation from the point of view of his age as well. We were discussing whether or not to apply for cardiac transplantation, but it turned out to be too late. If such a patient had been admitted to the institute where transplantation is actively carried out, he might have had a left ventricular assist device (LVAD) implanted and been ranked as status I in the transplantation registry, which means an urgent condition.

As a matter of fact, heart transplantation has been performed so far in 10 cases in Japan. Approximately 168 patients in total have applied to the Japanese Circulation Society transplantation sub committee, as of March 2001. Approximately 30 patients have died during the waiting period for elective transplantation. Eighty percent of these had DCM. Such patients can thus die without LVAD even while waiting for transplantation. In all, about 50% die in a year, and approximately 80% survive even in the presence of LVAD.

Anyway, the most serious problem is that there are very few organ donors available. Only a limited patients who undergo transplantation find themselves in the media spotlight. In reality, most patients die while waiting for transplantation.

Dr. Ogawa: As just mentioned, there are many patients with severe refractory heart failure, who die while waiting for cardiac transplantation. Our present patient might also have been a candidate for another form of non-drug therapy, *i.e.*, biventricular pacing. In this recently introduced treatment for heart failure, improvement of the cardiac function is sought by narrowing the QRS interval by pacing from both the right and left ventricles with a pacemaker, particularly in patients with a very wide QRS interval seen on ECG. What do you feel, Dr. Mitamura?

Dr. Mitamura: The method that Dr. Ogawa just referred to is called re-synchronization therapy; a lag of synchronism between the left and right ventricles induces abnormal motion of the interventricular septum; when the left ventricle contracts, for example, the interventricular septum protrudes into the right ventricle. To avoid this, innovations, such as simultaneous excitation and contraction of the right and left ventricles with a pacemaker have been introduced.

However, the present patient had a right bundle branch block, so his right ventricle in any event probably contracted later than his left ventricle. So, while there is the possibility that he would have felt slight relief with pacing of the right ventricle, the probability of improvement of his cardiac status is indeed rather limited, even if left ventricular pacing had been performed with a pacemaker introduced into the coronary sinus.

Table 3 Autopsy Finding

1. Dilated cardiomyopathy
   - A. Dilatation of the bilateral ventricles, severe
     Endocardial fibroelastosis
     Diffuse fibrosis in the left ventricle
   - B. Fibrinous fibroelastosis
   - C. Congestion of the lung
   - D. Congestion of the liver
   - E. Pleural effusion (left, 850 ml)
     + Ascites (290 ml)
2. Rectal cancer
   - A. Moderately differentiated adenocarcinoma, mp, ly0, v1, INFγ
   - B. No invasion or metastasis
3. Acute pancreatitis, severe

Dr. Ogawa: In regard to the differential diagnosis, the pathological study would ultimately determine whether the DCM in this patient was primary or secondary. However, the possibility of primary hereditary cardiomyopathy was clinically considered to be high. Dr. Umezawa, could you please describe the findings in this patient at autopsy.

Dr. Umezawa (Pathology): I shall now describe the biopsy and autopsy findings in this patient (Table 3).

This is a heart biopsy slide prepared in April 1993 (Fig. 6). The myocardium is slightly hypertrophic and characterized by the presence of abundant collagen fibrils in the intermyocardial interstitial tissue. Thus, there was myocardial hypertrophy with interstitial fibrosis.

The heart weighed 450 g, which represented an increase over the normal heart weight of 300 g. Marked dilatation of both the ventricles was observed (Fig. 7). The left ventricular wall was 0.9 cm thick (normal at autopsy, 1.5 cm). Thus, there was considerable thinning of the ventricular wall. The right ventricular wall was 0.3 cm thick (normal, 0.3–0.4 cm at autopsy). Therefore, the right ventricle showed slight thinning. There was also fibrinous pericarditis and endocardial fibroelastosis.

Histologically, (1) there were no inflammatory changes, (2) there was no evidence of any granuloma suggestive of cardiac sarcoidosis, and (3) diffuse myocardial fibrosis was present (Fig. 8A, B).

Mallory's staining was conducted to show the proportions of the myocardial fibers and collagen fibrils (Fig. 8C, D). The myocardial fibers were stained red and the collagen fibrils blue by the stain. The myocardial fibers were very coarse, and the collagen fibrils filled the spaces between the myocardial fibers. Poor contractility of the wall observed by echocardiography was supported by the histological findings – myocardial fibers which are essential for contraction of the muscle were replaced by collagen fibrils, which explained the hypokinesia of the myocardial wall observed clinically.

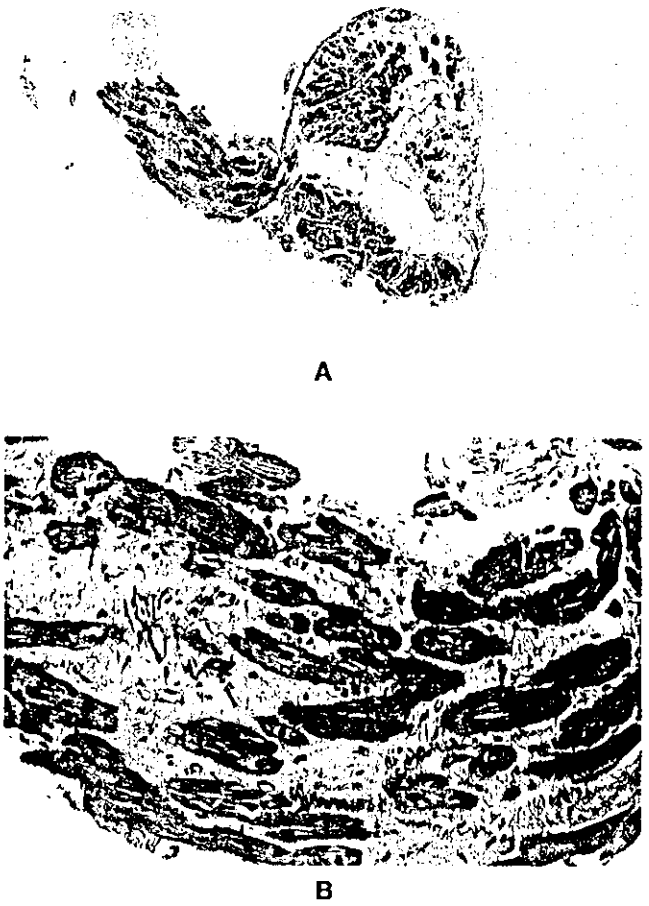

Fig. 6 Histological findings of the heart biopsy specimen. H.E. staining. Original magnification, A. ×40, B. ×200.

Vacuolar degeneration around the nuclei and the disappearance of the violet color reflecting myocardial degeneration and deficit are shown by PTAH staining (Fig. 8E). The myocardial fibers disappeared singly, and not in bundles, while fibers replaced by collagen fibrils showed hyperplasia. There was no complicated arrangement. The deficit and hypertrophy of the myocardial fibers were marked. Based on these findings, the patient's condition was diagnosed as DCM.

In addition, the lungs were edematous and severe hepatic congestion was observed; 850 ml of pleural fluid was found on the left side and 0 ml on the right side. In the right lung, complete adhesion of the parietal pleura and visceral pleura, which was probably consequent to the traffic accident, was observed.

A second remarkable finding was the presence of advanced cancer of the rectum. Since this was detected at autopsy, it was a latent carcinoma. It was a moderately differentiated adenocarcinoma, which had infiltrated up to the tunica muscularis propria. Slight venous invasion was observed. There was no infiltration to the bladder or other organs and no metastasis to other organs. Therefore, there was presumably no causal relationship between the rectal cancer and the patient's fatal course.

Fig. 7 Severe dilation of the right ventricle.

Dr. Yoshikawa: I got the impression that the histologically observed fibrosis was prominent, considering that this was a case of DCM. The tissue sample may have been collected from the site of fibrosis around the interventricular septum, which showed poor contraction echocardiographically. Administration of a β-blocker was attempted in this patient, but the heart failure deteriorated. Such patients often show severe interstitial fibrosis on histological examination. It is therefore noteworthy that DCM patients who have not respond satisfactorily to a β-blocker have also showed severe interstitial fibrosis on histology.

A β-blocker along with an ACE inhibitor is recommended prior to considering cardiac transplantation. Efforts were made with this patient, but introduction of the drug in this case was not successful. It is important to note that patients who do not tolerate β-blockers have a very poor prognosis.

Dr. Ogawa: This patient had mainly left heart failure, of course, but right heart failure was also a prominent clinical feature. In many cases with general DCM, the left cardiac system is mainly affected, and secondary pulmonary hypertension causes right heart failure. In this patient, however, the biopsy and autopsy findings revealed that the changes in the right ventricle were almost as marked as those in the left ventricle.

Dr. Umezawa: In this patient, fibrosis of the right ventricular wall was diffuse and severe. The dilatation of the right ventricle was slightly greater than that of the left ventricle.

Dr. Ogawa: This patient's condition was familial. Dr. Yoshikawa, could you please explain the characteristics of hereditary cardiomyopathy? One more thing I want

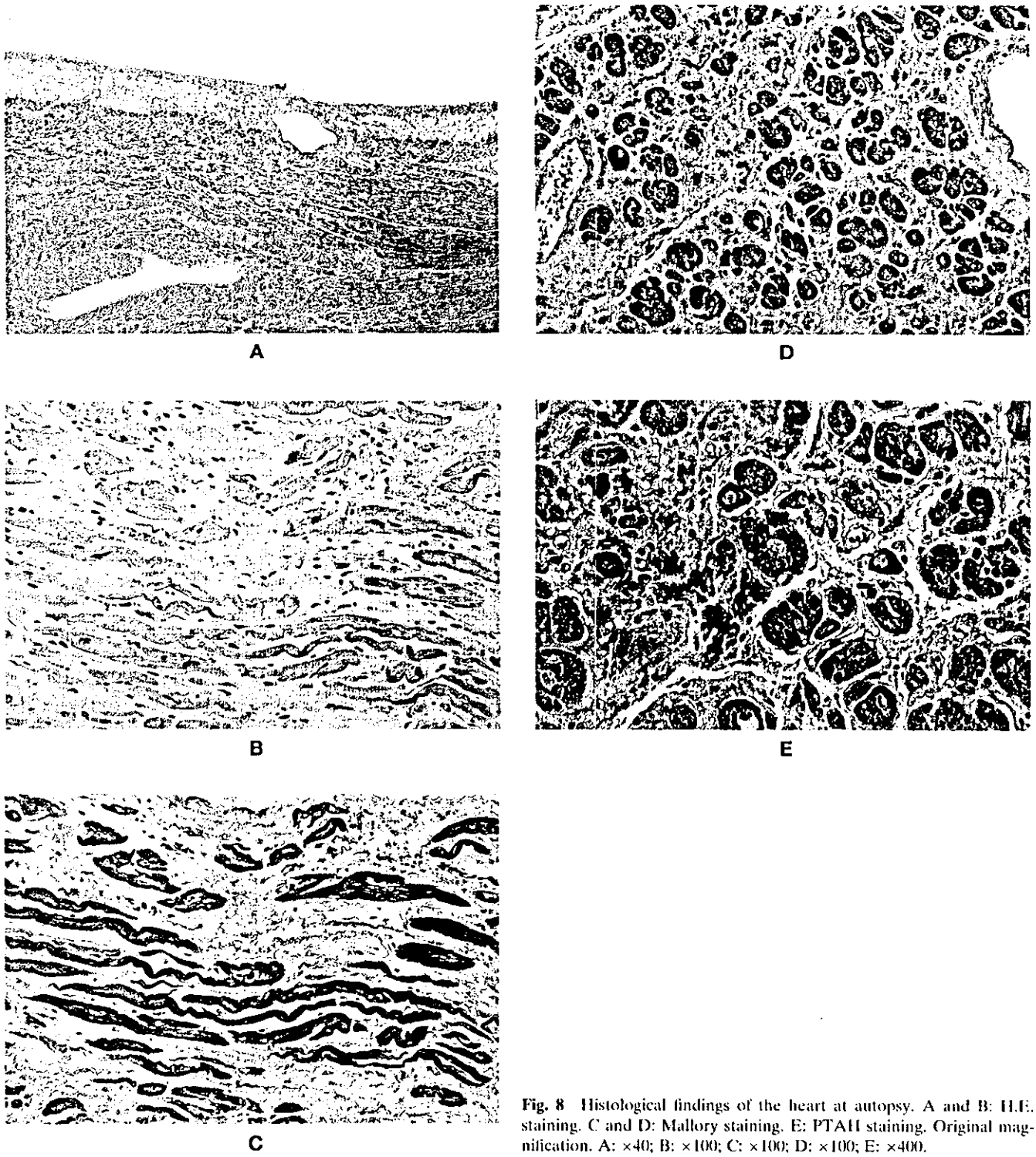

Fig. 8 Histological findings of the heart at autopsy. A and B: H.E. staining. C and D: Mallory staining. E: PTAH staining. Original magnification. A: ×40; B: ×100; C: ×100; D: ×100; E: ×400.

to ask is whether there is any basis for considering DCM as an autoimmune disease. It is possible that both the right and left ventricles are affected when autoantibodies directed against the myocardium are present.

Dr. Yoshikawa: No specific description has been made in terms of the clinical features of hereditary DCM. Many cases of hereditary hypertrophic cardiomyopathy have been reported, with a variety of gene mutations. As for the genetic mechanism responsible for the development of DCM, however, only a limited number of cases have been reported. Several proteins which support the contractile elements, including titin, are responsible for the development of DCM.

Basically, autoimmune cardiomyopathy in animal experiments shows the following pattern: the right ventricle is dilated and cardiomyopathy mimicking arrhythmogenic right ventricular cardiomyopathy (ARVC) develops. It remains unknown whether or not autoimmunity was involved in the present patient, but it would have been of interest to study this aspect.

Dr. Umezawa: There was no morphological evidence of viral infection. I wonder whether viruses are related to autoimmunity.

Dr. Yoshikawa: It has generally been considered that viral infection causes acute myocarditis, in which cellular immune mechanisms are activated. When the cellular membrane becomes disrupted, various proteins are exposed. If some proteins are presented persistently on antigen presenting cells, some antibodies will be produced, causing chronic and persistent damage to the myocardium.

Dr. Ogawa: Could you please give your concluding comments on the case, Dr. Mitamura?

Dr. Mitamura: Of the many patients who die of heart failure, about half die a sudden death, and the remaining die of progressive heart failure. The present patient followed a fairly atypical course; the heart function was considerably poor; even as far back as in 1997, the patient had already reached the level where patients are generally expected to survive for only 1 or 2 years. Of the various treatment methods introduced recently, the use of a β-blocker was initiated in this patient, but unfortunately, it proved to be ineffective. However, pimobendan, a PDE inhibitor, also known as a calcium sensitizer, exerted some beneficial effect, and the patient himself felt significant improvement in his condition. The heart function was very poor, but it remained stable for some time. Death in cases of heart failure is frequently associated with infection, but we often encounter patients, like the present patient, in whom death occurs as a consequence of rapid deterioration of renal function.

One remarkable characteristic in this patient was that the changes in the right ventricle were also marked. The arrhythmia recorded in his case could easily explained by this finding. The serum BNP level was also markedly increased. These findings suggest widespread lesions in the myocardium. The elevation of the BUN level was believed to be influenced by the use of a diuretic, and it is known to be very difficult to use diuretics in the presence of right heart failure. These patients easily slip into dehydration. This also seems to have made the treatment of this patient more difficult.

In conclusion, heart transplantation could have been considered, but my impression is that transplantation would have been a difficult proposition in this case, because his pulmonary function was also compromised as a result of his traffic accident.

Dr. Ogawa: Thank you very much for your comments.

The patient discussed in today's CPC had refractory heart failure. According to the text book, 50% of heart failure patients die within 5 years of the diagnosis. Thus, it is a very serious disease; patients usually die within 2 to 3 years, on average, after the onset of heart failure. Despite this bleak prognosis, owing to the currently available methods of treatment, our patient lived for 8 years after the diagnosis of heart failure. If heart transplantation were introduced more aggressively in clinical cases, it could be lifesaving.

ACADEMIC PRESS

Biochemical and Biophysical Research Communications 293 (2002) 61–71

BBRC

www.academicpress.com

Lack of matrix metalloproteinase (MMP)-1 and -3 expression in Ewing sarcoma may be due to loss of accessibility of the MMP regulatory element to the specific fusion protein in vivo

Hiroki Yabe,[a,b] Mariko Fukuma,[a] Fumihiko Urano,[a] Koichi Yoshida,[c] Shingo Kato,[d] Yoshiaki Toyama,[b] Jun-ichi Hata,[a] and Akihiro Umezawa[a,*]

[a] *Department of Pathology, Keio University School of Medicine, 35 Shinanomachi, Shinjuku-ku, Tokyo 160-8582, Japan*
[b] *Department of Orthopaedics, Keio University School of Medicine, 35 Shinanomachi, Shinjuku-ku, Tokyo 160-8582, Japan*
[c] *Department of Molecular Biology, Cancer Research Institute, School of Medicine, Sapporo Medical University, S-1, W-17, Chuoku, Sapporo 060-8556, Japan*
[d] *Department of Microbiology, Keio University School of Medicine, 35 Shinanomachi, Shinjuku-ku, Tokyo 160-8582, Japan*

Received 19 February 2002

Abstract

Ewing sarcoma is a malignant bone and soft tissue tumor of children and young adults, which is known to be highly aggressive and invasive. It expresses specific chimeric genes (EWS-FLI-1, EWS-ERG, EWS-ETV1, and EWS-E1AF), the 3′ portions of which are all members of the ETS family. ETS-related proteins, such as FLI-1, ERG, and E1AF, transactivate the promoters of matrix metalloproteinase (MMP) genes, which play important roles in the processes of invasion and metastasis. Therefore, we hypothesize that the Ewing sarcoma-specific chimeric genes also transactivate the MMP genes, contributing to the tumor's invasiveness and propensity for metastasis. To verify this hypothesis, we investigated the expression of MMPs in eight Ewing sarcoma cell lines. Surprisingly, MMP-1 and MMP-3 were not expressed at all in any of the cell lines. MMP-9 was expressed in four out of the eight cell lines, and MMP-2 and MT1-MMP in all of the cell lines. Ewing sarcoma-specific chimeric genes have been shown to transactivate the promoter of the MMP-1 gene by the reporter assay, and bind to the putative recognition sites in the MMP regulatory elements by the gel shift assay. However, an in vivo formaldehyde cross-linking study revealed that the chimeric protein did not bind to the predicted ETS recognition sites in the regulatory elements of the MMPs. These results indicate that the absence of the MMP expression in the tumor cells is at least in part due to the loss of accessibility of the ETS recognition sites in the regulatory elements of the MMP genes. Therefore, we should be careful before theorizing simply that a putative binding site is essential for the transcription of critical genes, since the binding of this fusion protein was found to be modulated in tumor cells in this study.

Keywords: Ewing sarcoma; ETS; E1AF; RNA binding protein

Ewing sarcoma, one of the most common malignant tumors of children and young adults, is an aggressive osteolytic tumor with a marked propensity for dissemination [1] and has neurogenic potential [2]. Recently, many human sarcomas have been reported to contain characteristic chromosomal translocations, which generate specific chimeric genes [3–5]. Ewing sarcoma is characterized by a specific chromosomal translocation, t(11; 22) [6,7], through which the EWS-FLI-1 chimeric gene is generated [8]. FLI-1, a component of the chimeric gene, is a member of the ETS family of transcription factors. Other members of the ETS family of genes, ERG, ETV1, and E1AF, are also fused to EWS through t(21; 22), t(7; 22), and t(17; 22), respectively [9–12], in Ewing sarcoma.

Ewing sarcoma-specific chimeric genes contain members of the ETS family on their 3′ side and are considered to play important roles in oncogenesis and malignancy. The target genes for these chimeric genes remain unclear. But, matrix metalloproteinase (MMP)-3

* Corresponding author. Fax: +81-3-3353-3290.
E-mail address: umezawa@1985.jukuin.keio.ac.jp (A. Umezawa).

0006-291X/02/$ - see front matter
PII: S0006-291X(02)00129-8

(stromelysin-1) has been suggested to be a direct target of EWS-FLI-1 by representational difference analysis [13]. The promoters of human MMP-1 (collagenase-1) and MMP-3 have been reported to be transactivated by the c-ETS-1 and c-ETS-2 genes [14,15]. In addition, ERG transactivates MMP-1 [16], and E1AF transactivates MMP-1, MMP-3, and MMP-9 (gelatinase B) [17].

Based on these findings, we speculate that Ewing sarcoma-specific chimeric genes can transactivate MMP-1, MMP-3, and MMP-9 through their binding to putative recognition sites in their regulatory elements, and contribute to the invasiveness and propensity for metastasis of Ewing sarcoma. Although there are a few reports on the expression patterns of the MMP genes in osteosarcoma [18] and chondrosarcoma [19], MMP gene expression in Ewing sarcoma has not yet been investigated. In this report, we investigated the transcriptional activation of the MMP-1, MMP-3, and MMP-9 promoters by Ewing sarcoma-specific fusion products, and the expression patterns of the MMPs, including MMP-1, MMP-2 (gelatinase A), MMP-3, MMP-9, TIMP-1, TIMP-2, and MT1-MMP, in Ewing sarcoma cell lines and primary Ewing sarcoma tumors. Surprisingly, Ewing sarcoma cells did not express MMP-1 and -3. However, they did express MMP-2 and -9 and MT1-MMP. Lack of MMP-1 and -3 expression seems to result from the loss of accessibility of the ETS recognition sites in the regulatory elements of the MMPs to the Ewing sarcoma-specific chimera.

Materials and methods

Tumors and cell lines. Five surgical specimens of Ewing sarcoma/peripheral primitive neuroectodermal tumor (PNET) were obtained from Japanese patients. The patient characteristics are summarized in Table 1B. The tumors were diagnosed as Ewing sarcoma or PNET based on the clinical and pathological findings. Two new Ewing sarcoma cell lines, K-EW2 and K-EW3, were established from the tumor specimens of two patients (Table 1A). The tumor specimens were minced and cultured in dishes of Dulbecco's modified minimum essential medium (GIBCO) in the presence of 10% fetal bovine serum (GIBCO). Both lines grew stably for more than 30 passages. In addition to these two newly established cell lines, six previously established Ewing sarcoma cell lines (NCR-EW2 [20], NCR-EW3 [20], SK-ES1, SCCH-196 [21], W-ES [22], and K-EW1 [23]) are being maintained in our laboratory (Table 1A). SK-ES1 was purchased from the American Type Culture Collection (ATCC, Rockville, MD, USA). MRC-5, which represents immortalized cell clones from transformed human fibroblasts [24], used as control cells, is also maintained in our laboratory. The cells were cultured at 37 °C in Dulbecco's modified minimum essential medium in the presence of 10% fetal bovine serum and 5% CO_2 in 25-cm^2 culture flasks. The cultured cells were then suspended in phosphate-buffered saline containing 0.05 M EDTA, without calcium and magnesium.

Reverse transcription and polymerase chain reaction (RT-PCR), and RNA blot analysis. Total RNAs from the tumors and cell lines were extracted by the guanidinium thiocyanate method, followed by centrifugation in cesium chloride solutions [25] or ISOGEN (Nippon Gene, Tokyo). The surgical specimens were minced with a small stick in a microcentrifuge tube. Complementary DNA was generated using the first-strand cDNA synthesis kit (Pharmacia Biotech, Uppsala). Approximately 1–5 μg of total RNA was transcribed. Polymerase chain reaction (PCR) was carried out in a 100 μl reaction mixture containing 1–7 μl of the cDNA template, 200 mM of deoxynucleotide triphosphates, 0.5 mM of each oligonucleotide primer, and 2.5 units of Taq polymerase in 10 mM Tris–HCl buffer (pH 8.8) containing 50 mM KCl, and 1.5 mM $MgCl_2$. The oligonucleotide primers used for the PCR were based on the sequences of ESBP-1 (EWS specific) and ESBP-2 (FLI-1 specific) [26]. PCR was performed in 35 cycles under the following protocol: denaturation step at 94 °C for 1 min, annealing at 65 °C for 1 min and elongation step at 72 °C for 1 min. The amplified products were analyzed on 1% agarose gel.

For the RNA blot analysis, 10 μg of total RNA was electrophoresed on 1.0% agarose gel, transferred to a nylon membrane and hybridized with a cDNA probe radiolabeled with [α-^{32}P]dCTP, by the random-primer method, at 65 °C for 14–16 h in a buffer containing 5× SSPE, and 5× Denhardt's solution. The blots were washed with 2× SSC containing 1% SDS at room temperature and at 65 °C. Final washings were done with 0.1× SSC containing 0.1% SDS at 65 °C. The blots were exposed to X-ray films using an intensifying screen.

Table 1
Description of Ewing/PNET cell lines and primary Ewing/PNET tumors in patients

Case	Cell line	Age/sex	Surgical samples	Origin	Diagnosis	Fusion transcript
(A) *Cell lines*						
1	NCR-EW2	13 yr/male	ST433	Pelvis (EO)	EWING	EWS exon7-FLI-1 exon5
2	SK-ES1	18 yr/male	–	unknown	EWING	EWS exon7-FLI-1 exon5
3	SCCH196	16 yr/female	ST854	Upper arm (EO)	EWING	EWS exon7-FLI-1 exon6
4	K-EW2	18 yr/male	KST1420	Fibula (O)	EWING	EWS exon7-FLI-1 exon6
5	K-EW3	13 yr/male	KST1446	Rib (O)	EWING	EWS exon7-FLI-1 exon6
6	K-EW1	15 yr/male	KST1166	Pelvic cavity (EO)	EWING	EWS exon7-ERG exon9
7	W-ES	14 yr/male	–	Chest wall (EO)	EWING	EWS exon7-ERG exon9
8	NCR-EW3	10 yr/male	ST480	Chest wall (EO)	EWING	EWS exon7-E1A-F
(B) *Primary tumors*						
		13 yr/male	ST433	Pelvis (EO)	EWING	EWS exon7-FLI-1 exon5
		30 yr/male	KST652	Thigh (EO)	PNET	EWS exon7-FLI-1 exon5
		24 yr/male	KST1461	Tibia (O)	EWING	EWS exon7-FLI-1 exon6
		15 yr/male	KST1166	Pelvic cavity (EO)	EWING	EWS exon7-ERG exon 9
		10 yr/male	ST480	Chest wall (EO)	EWING	EWS exon7-E1A-F

(O) Osseous; (EO) Extraosseous.

CAT assay. Chloramphenicol acetyltransferase (CAT) reporter genes driven by promoters of type I collagenase, stromelysin, and 92 kDa type IV collagenase genes were co-transfected into human HeLa cells containing a Ewing sarcoma-specific chimeric gene (EWS-FLI-1, EWS-ERG, and EWS-E1AF) expression vector and pACT-β gal plasmid as a reference by the lipofection method. After 48 h, cell extracts were prepared, and the CAT and β-galactosidase activities were assayed by a standard procedure [27,28].

Subcloning of the target genes of EWS-FLI-1 using the in vivo formaldehyde cross-linking technique, and hybridization analysis. The cell cultures of Ewing sarcoma cells (NCR-EW2), labeling and formaldehyde fixation, immunoprecipitation of in vivo-fixed chromatin fragments using an anti-human FLI-1 antibody (Santa Cruz Biotechnology, sc-356) or anti-human IgG antibody as a control, purification of the immunoprecipitated DNA, and linker-modified PCR amplification were performed according to the methods described by Orlando and Paro [29]. Subcloning of DNA was carried out using pGEM-T Vector Systems (Promega, Madison, WI, USA).

About 30 ng of amplified DNA probes immunoprecipitated by the anti-human FLI-1 antibody was labeled using an oligonucleotide random-primed DNA synthesis kit with [α-^{32}P]dCTP (specific activity, 3000 Ci/mmol; Amersham). Slot-blot analyses were performed with a slot-type dot blotting apparatus (Bio-Rad) equipped with nylon filters. About 100 ng of template DNA was loaded onto a nylon membrane, and hybridized with labeled DNA probes at 65 °C for 14–16 h in a buffer containing 5× SSPE, and 5× Denhardt's solution. The blots were washed with 2× SSC containing 1% SDS at room temperature and at 65 °C. Final washings were done with 0.1× SSC containing 0.1% SDS at 65 °C. The blots were exposed to a phosphoimaging plate and image quantitation was performed using a phosphoimaging apparatus.

Gel mobility shift assay. Gel mobility shift assay was performed as described previously [30,31]. The annealed double-stranded oligonucleotide was labeled by the fill-in reaction of Sequenase version 2 (US Biochemicals), in the presence of radioactive dCTP on the AGCT extensions added to the oligonucleotide. The upper strand of the oligonucleotides (Col I-88 ets S: tcgaATCAAGAGGATGTTATAA) containing the ets site (underlined) of human collagenase (MMP-1) promoter was used. Nuclear proteins extracted from Ewing sarcoma cells (NCR-EW2) were prepared as described previously [30]. Nuclear protein–DNA binding reactions were performed in binding buffer containing 40,000 cpm of a ^{32}P-labeled probe, 15 μg of nuclear proteins, 10 μg of poly(dA-dT), for 10 min at 4 °C in the presence of an excess or absence of unlabeled intact or mutated oligonucleotide (100×, 250× and 500×). In one reaction, a specific antibody raised against the FLI-1 protein (Santa Cruz Biotechnology, sc-356) was used. The protein–DNA complexes were analyzed on a 5% polyacrylamide gel containing 0.4× TBE. The gel was dried and autoradiographed.

Results and discussion

Generation of new Ewing sarcoma cell lines

We established two new cell lines (K-EW2 and K-EW3) from the tumor specimens of Ewing sarcoma patients (Figs. 1A–D). Histology of the primary tumors showed small round cells with round to ovoid nuclei. Some tumor cells stained positive for the periodic acid–Schiff reaction, which were digested with diastase. These tumor cells were not arranged in any particular configuration, such as in the form of rosettes. K-EW2 cells grew to give a fibrocytic appearance, while K-EW3 cells grew as a polygonal cell sheet with the formation of cell aggregates at the center. In both of these cell lines, the EWS-FLI-1 chimeric gene was detected by RT-PCR (Fig. 1E).

Expression of the MMP and related genes in Ewing sarcoma cell lines and primary tumors

We investigated the expression of the MMP and related genes in Ewing sarcoma, since (a) specific fusion genes between EWS and ETS-related genes are present in Ewing sarcoma; (b) the MMP-1, -3, and -9 genes are activated by ETS-related oncogenes through binding to their regulatory elements; and (c) the MMP genes are candidate target genes for the specific fusion genes (Fig. 2 and Table 2A). Eight human tumor cell lines established from Ewing sarcoma cells, including the two new cell lines, K-EW2 and K-EW3, were examined for their expression of MMP-1, -2, -3, and -9, and MT1-MMP. MMP-1 and MMP-3 were not expressed in any of the Ewing sarcoma cell lines tested, while they were in MRC-5 used as the positive control (Fig. 2 and Table 2A). MMP-9 was expressed in four out of the eight cell lines (Fig. 2D). MMP-2, MT1-MMP, TIMP-1, and TIMP-2 were expressed in almost all the cell lines (Figs. 2C, E and F).

To eliminate the possibility of bias in the expression pattern of the MMP genes in Ewing sarcoma cell lines arising through the establishment of the cell lines from primary tumors, five human surgical specimens obtained from patients of Ewing sarcoma were examined for their expression of MMP-1, -2, -3, and -9, and MT1-MMP (Fig. 3 and Table 2B). MMP-1 and MMP-3 were not expressed in any of the Ewing sarcoma tumor specimens (Figs. 3A and B). MMP-2 and MT1-MMP were expressed in almost all, while MMP-9 was expressed in only a few of the specimens (Figs. 3C–E). This expression pattern of MMPs in the Ewing sarcoma tumor specimens was consistent with that in cell lines.

Transcriptional activation of the promoter of MMP-1 by Ewing sarcoma-specific chimeric genes

The promoters of MMP-1 and MMP-3 are known to be transactivated by ETS-related genes, including ERG and E1AF. However, our results show that MMP-1 and MMP-3 are not expressed in Ewing sarcoma cell lines and tumors. We hypothesize that this lack of expression of the MMP-1 and -3 genes is due to the loss of transcriptional activation of the promoters of MMP-1 and MMP-3 by the chimera genes. Therefore, we analyzed the transcriptional activation by the chimeric genes, i.e., EWS-FLI-1, EWS-ERG, and EWS-E1AF, of the promoters of MMP-1 and MMP-3. All the three chimeric genes tested clearly induced transcriptional activation on the MMP-1 promoter (−517/+63), although to

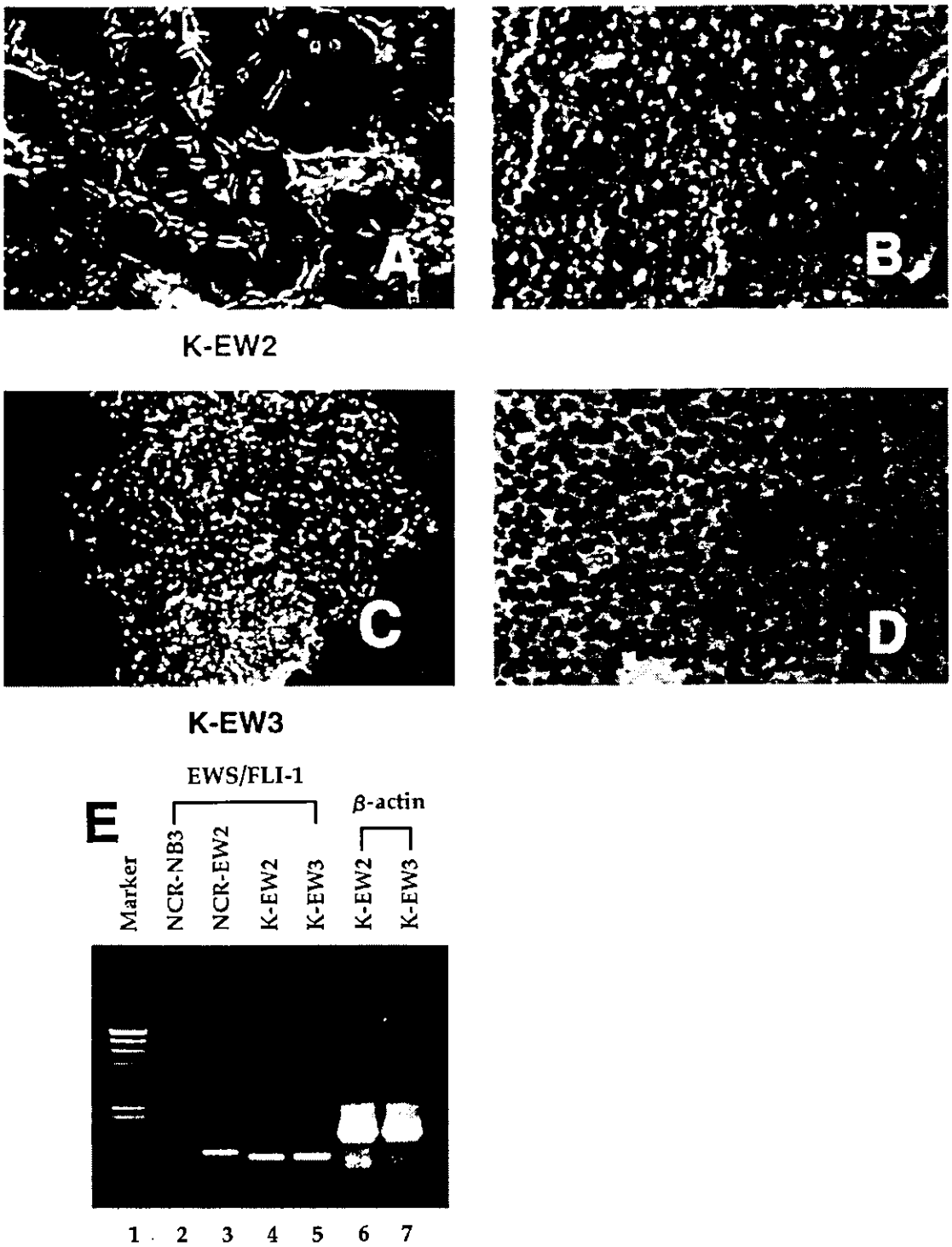

Fig. 1. Generation of two new Ewing sarcoma cell lines, K-EW2 and K-EW3, with the specific chimera gene, EWS-FLI1. (A) Phase-contrast photograph of K-EW2 cells in culture at a low cell density. The cells were fibrocytic in morphology (100×). (B) Histological appearance of the original tumor of K-EW2 cells. Small round tumor cells showing diffuse proliferative activity. Neither the Homer–Wright-type rosette formation nor that of any other specific structure was noted (HE, 100×). (C) Phase contrast photograph of K-EW3 cells. The cells grew as an attaching aggregate or a colony. (D) Histological appearance of the original tumor of K-EW3 (HE, 100×). (E) RT-PCR analysis of a cell line of Ewing sarcoma. Total RNAs were analyzed by RT-PCR using EU-1 (EWS specific) and EU-2 (FLI-1-specific)-sequence-based primers. The EWS-FLI-1 fusion gene was detected in both K-EW2 and K-EW3 cell lines (311 bp, lanes 4 and 5). The NCR-EW2 cell line, which contains EWS-FLI-1 fusion transcripts, was used as the positive control for the PCR reaction (377 bp, lane 3). NCR-NB3 cell line, established from a neuroblastoma, was used as the negative control (lane 2). β-actin gene is also detected in the K-EW2 and K-EW3 cell lines (868 bp, lanes 6 and 7).

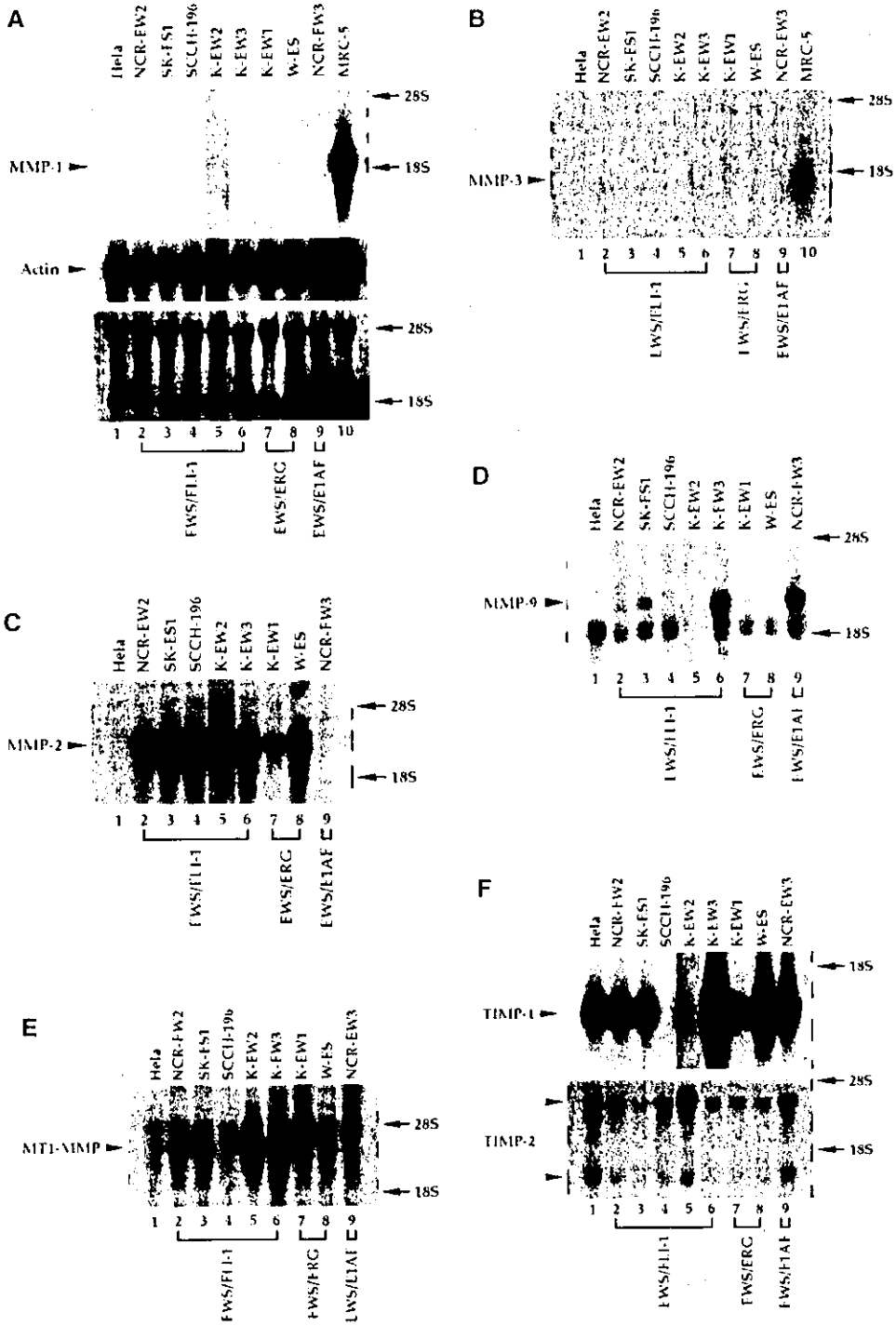

Fig. 2. Expression of MMPs and TIMPs in Ewing sarcoma cell lines. Northern blot analysis of MMP-1 (A), MMP-3 (B), MMP-2 (C), MMP-9 (D), MT1-MMP (E), and TIMP-1 and -2 (F) in Ewing sarcoma cells and control cells. Lanes 2–6: The cell lines established from Ewing sarcomas which have EWS-FLI-1, NCR-EW2, SK-ES1, SCCH196, K-EW2, and K-EW3. Lanes 7 and 8: K-EW1 and W-ES cells with EWS-ERG. Lane 9: NCR-EW3 with EWS-E1AF. HeLa cells (lane 1) and MRC-5 cells (lane 10) served as controls. The amount of total RNA was checked by the level of expression of the β-actin gene (A, middle part) and, 18S and 28S rRNA stained with methylene blue (A, lower part).

different levels (Fig. 4A). Thus, MMP-1 is not expressed in Ewing sarcoma cells and primary tumors, even though Ewing sarcoma-specific chimeric genes, including EWS-FLI-1 and EWS-ERG, can transactivate the promoter of MMP-1. In contrast, EWS-FLI-1 and EWS-ERG have a tendency to activate the MMP-3 promoter, although their activities are no more than those in the MMP-1 promoter (Fig. 4B).

Table 2
MMP and TIMP gene expressions in Ewing sarcoma/PNET cell lines

Type of MMPs and TIMPs	ets site	Gene expression									
		HeLa	EWS/FLI-1					EWS/ERG		EWS/E1AF NCR-EW3	MRC-5
			NCR-EW2	SK-ES1	SCCH196	K-EW2	K-EW3	K-EW1	W-ES		
(A) *PNET cell lines*											
MMP-1	+	−	−	−	−	−	−	−	−	−	+
MMP-2	−	−	+	+	+	+	+	+	+	−	
MMP-3	+	−	+	+	−	−	+	−	−	+	+
MMP-9	+	−	+	+	−	−	+	−	−	+	
MT1-MMP	+	−	+	+	−	+	+	+	+	+	
TIMP-1	+	+	+	+	−	−	+	+	+	+	
TIMP-2	−	+	+	+	+	+	+	+	+	+	

Type of MMPs and TIMPs	ets site	Gene expression					
		EWS/FLI-1			EWS/ERG	EWS/E1AF	MRC-5
		ST433	KST652	KST1461	KST1166	ST480	
(B) *PNET tumors*							
MMP-1	+	−	−	−	−	−	+
MMP-2	−	+	+	+	−	+	
MMP-3	+	−	−	−	−	−	+
MMP-9	+	+	−	−	−	−	
MT1-MMP	+	+	+	+	+	−	

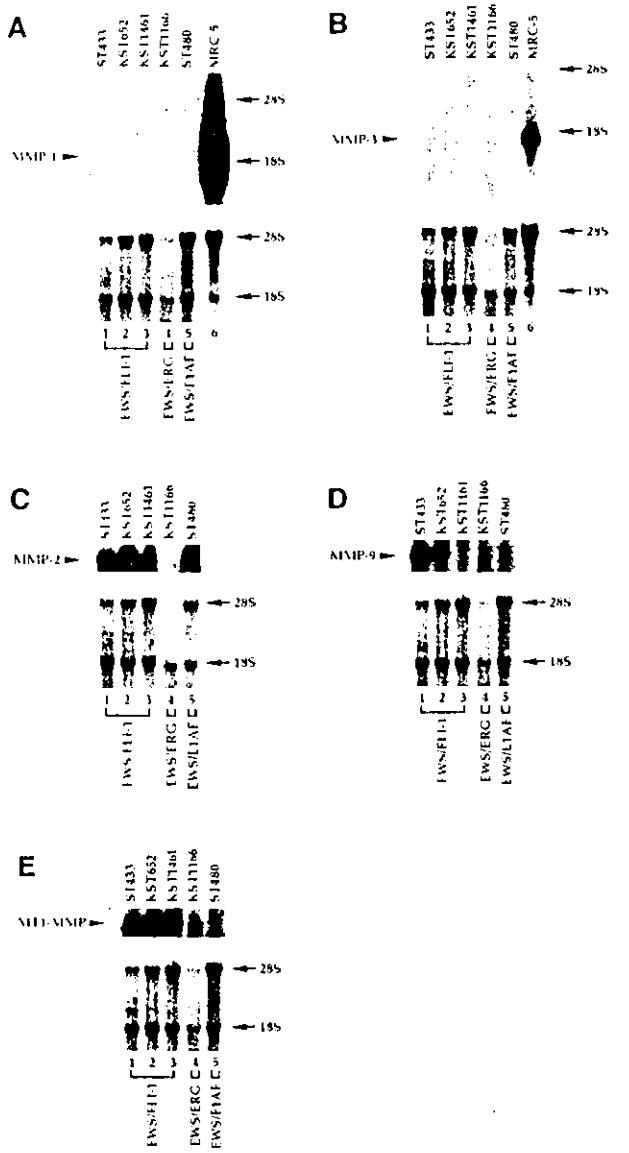

Fig. 3. Expression of MMPs in Ewing sarcoma specimens. Northern blot analysis of MMP-1 (A), MMP-3 (B), MMP-2 (C), MMP-9 (D) and MT1-MMP (E) in Ewing sarcoma specimens. Total RNA was isolated from ST433, KST652, and KST1461 (lanes 1–3) which have the EWS-FLI-1 fusion transcript; KST1166 (lanes 4) with the EWS-ERG chimeric gene; ST480 (lane 5) with the EWS-E1AF chimeric transcript. MRC-5 cells served as the control (A and B, lane 6). The amount of total RNA was checked by the level of expression of 18S and 28S rRNA stained with methylene blue (lower part).

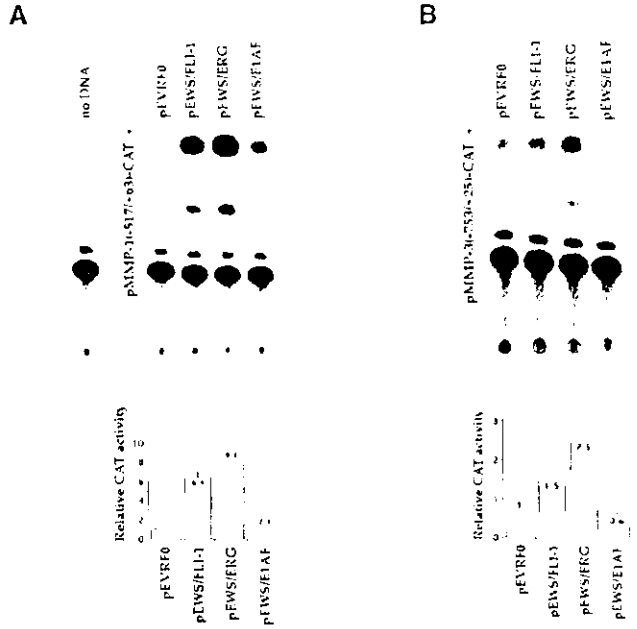

Fig. 4. Activation of MMP-1 and MMP-3 promoter activity by the EWS-FLI-1, EWS-ERG, and EWS-E1AF fusion proteins. Representative autoradiograms of CAT assays (upper part). By using the lipofection method, HeLa cells were co-transfected with 2 mg of the reporter plasmids (A: pMMP-1 (−517/+63); B: pMMP-3 (−753/+25)), 2 mg of internal control plasmids (actin-bgal) and 2 mg of empty vector (pEVRF0) or the expression vector of either EWS-FLI-1, EWS-ERG or EWS-E1AF driven by the cytomegalovirus (CMV) promoter. Cells were harvested 48 h after transfection, and the CAT activity was measured using a silica gel plate and visualized by autoradiography. After repeating the same experiments four and three times (A and B, respectively), the average and standard error of CAT activity corrected for variations in the internal control are indicated (lower part).

Loss of accessibility of the MMP regulatory element to the specific fusion protein in vivo

To elucidate the reason for the absence of MMP-1 expression despite the strong transcriptional activation of its promoter by the EWS-FLI-1 chimeric protein, we employed the in vivo formaldehyde cross-linking technique. With this technique, we investigated whether the EWS-FLI-1 chimeric protein binds to the ETS recognition sites in the regulatory elements of the MMP promoters in vivo. To determine whether the target sequences were precisely precipitated with the anti-FLI-1 antibody, we used Iti, Juyon, and Jugo, which have recently been isolated as target sequences (deposited in Genbank as AF177750, AF177751, and AF177752, unpublished observations). The signals of Iti, Juyon, and Jugo loaded on the nylon filter were enhanced reproducibly, indicating that the in vivo formaldehyde cross-linking and immunoprecipitation occurred precisely. In contrast, the signals of MMP-1, MMP-3, and MMP-9 promoter DNA were not enhanced when hybridized with the precipitated DNA, including the EWS-FLI-1 binding elements with the anti-FLI-1 antibody, as compared with that when hybridized with nonspecific DNA (Fig. 5A). Thus, the EWS-FLI-1 chimeric proteins did not bind to the promoters, including the predicted ETS recognition sites of MMP-1, MMP-3, and MMP-9, in Ewing sarcoma cells.

To determine whether the absence of in vivo binding of the Ewing sarcoma-specific chimeric proteins is due to the loss of the binding ability of the chimeric protein to the ETS recognition sites in the promoters, we performed the gel mobility shift assay. The signal of the

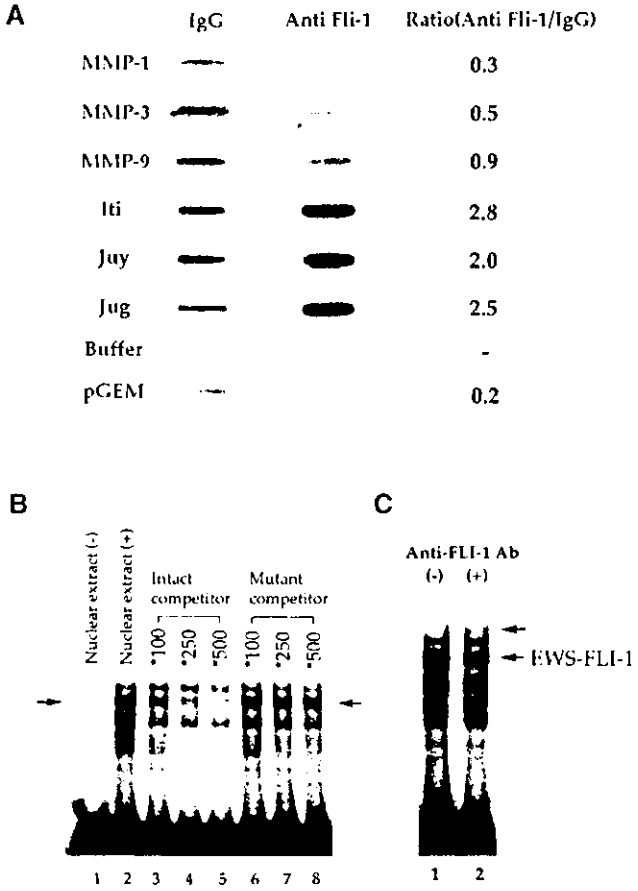

Fig. 5. Slot blot analysis of the DNA containing MMP-1, MMP-3, or MMP-9 regulatory elements and the gel shift assay. (A) DNA fragments containing the MMP-1 (−517/+63), MMP-3 (−9/−440), or MMP-9 (−670/+53) regulatory elements, were, respectively, applied to individual slots on a nylon filter. As positive controls, the DNA fragments (Iti, Juyon, and Jugo) cloned as including EWS-FLI-1 binding elements were applied onto individual slots on the same nylon filter. As negative controls, buffer only and pGEM vector only were applied onto the slots on the nylon filter. The loaded filter was hybridized with the DNA obtained by immunoprecipitation of cross-linked chromatin by anti-FLI-1 antibody and also with the anti-IgG antibody for comparison. The intensity of each of the signals enhanced by the FLI-1 antibody is calculated and shown on the right. Binding activity of a double-stranded oligonucleotide (Col I-88 ets) containing the ets site of the human collagenase (MMP-1) promoter detected by the gel shift assay. (B) Complexes were formed between the ^{32}P-labeled probe and nuclear proteins extracted from Ewing sarcoma cells (NCR-EW2). Lane 1: Probe alone; Lane 2: Probe and nuclear protein; Lanes 3–5: Competition with a 100-, 250-, or 500-fold molar excess of non-radioactive intact oligonucleotide; Lanes 6–8: Competition with a 100-, 250- or 500-fold molar excess of nonradioactive mutated oligonucleotide. (C) Lane 1: Probe and nuclear protein; Lane 2: Probe, nuclear protein, and specific antibody raised against the FLI-1 protein.

MMP-1 ET element was shifted with the addition of the nuclear extracts of Ewing sarcoma cells. This shifted signal was decreased by the intact competitor, but not by a mutant competitor (Fig. 5B). It was also supershifted by the FLI-1 antibody (Fig. 5C). These results suggest that the EWS-FLI-1 chimeric protein can bind to the predicted ETS element in vitro, and that there are no inhibitors which prevent the chimeric protein from binding in the nuclear extracts of Ewing sarcoma cells.

Expression of metalloproteinase genes in Ewing sarcoma

In this study, we have demonstrated for the first time metalloproteinase gene expression in Ewing sarcoma and Ewing sarcoma cell lines, including two newly established lines. A series of metalloproteinase genes and tissue inhibitors of metalloproteinases have been purified or cloned. Extensive effort has been expended on investigating the expression profiles of such genes in a variety of carcinomas, since the expression patterns or levels are reported to be directly linked to the biological properties of the tumor, such as its propensity for metastasis and invasiveness. Most cancer cells produce higher levels of metalloproteinases, as compared with their normal counterparts. The expression profiles of MMPs have been analyzed in carcinomas of the breast, thyroid gland, endometrium, and oral cavity. However, quantitative expression analyses of the metalloproteinases have not yet been performed in sarcomas [18,19]. In this study, we show that Ewing sarcomas express MMP-2, MMP-9, MT1-MMP, TIMP-1, and TIMP-2, but not MMP-1 or MMP-3. MMP-2 participates in the invasion by a carcinoma of the basement membrane, and is activated by MT1-MMP [32–34]. Activation and enhanced production of MMP-2 are detected in metastatic tumors of human thyroid carcinomas and human astrocytic tumors showing malignant transformation [35,36]. Similarly, the highly aggressive and invasive nature of Ewing sarcoma may be explained by the high level of expression of MMP-2 and MT1-MMP, which function cooperatively in the degradation of extracellular matrix.

Besides their pathological significance, the high expression levels of MMP-2, MT1-MMP, and TIMP in all the surgical specimens and cell lines of Ewing sarcoma examined evoked a possibility that EWS-FLI1 directly transactivates these genes. The regulation of expression of the MMP genes has been investigated at the mRNA level [37–42]. MT1-MMP is induced by v-src or erbB-2. MMP-2 and MMP-9 are regulated by integrins and E-cadherin, respectively. Hence, oncogenes and cell adhesion molecules are directly related to the expression levels of degradation enzymes of the extracellular matrix. Although the transcriptional regulation of such genes has not been elucidated yet, we cannot entirely deny the possibility that MMP-2, MT1-MMP, and TIMP are among the targets for the fusion protein.

Possible mechanism underlying the lack of MMP expression

The lack of expression of MMP-1 and -3 in Ewing sarcoma found by us was unexpected, since sarcomas originates from undifferentiated mesenchymal cells.

Most mesenchymal cells such as fibroblasts, synovial cells, and chondrocytes, which are of mesodermal origin, express MMP-1 and -3 at a high level. Furthermore, the MMP-1 and -3 genes are transactivated through the ETS recognition sites in their regulatory elements, and Ewing sarcoma has specific chimeric genes between those for EWS and ETS transcription factors. Therefore, the MMP-1 and -3 genes were expected to be expressed in Ewing sarcoma, which was not the case.

The chromatin immunoprecipitation method employed in this study provides information on the target genes of transcriptional factors in vivo. We employed this method for two purposes: (a) for in vivo binding of the fusion gene to their putative recognition sequences in the regulatory elements of MMP-1 and -3; (b) isolation of the target genes or sequences of the fusion gene. So far, MMP-3, cytochrome P450-F1, cytokeratin 15, EAT-2, and manic fringe have been suggested as target genes of the Ewing sarcoma-specific fusion protein [13,43,44]. However, as shown in this study, MMP-3 was not a target gene of the fusion protein of Ewing sarcoma in vivo. This is based on the evidence that MMP-3 was not expressed in any of the surgical specimens and cell lines of Ewing sarcoma, and EWS-FLI1 did not bind to the MMP-3 regulatory element in vivo. In addition to MMP-3, the transcriptional activation, which was detected by a transient transfection method, by the fusion genes of the MMP-1 regulatory element was not associated with the expression of the MMP-1 gene in vivo, either. Lack of binding of the fusion gene product in vivo to the regulatory elements of these two genes was rather surprising, since binding ability of the fusion protein to the ETS recognition sequence was observed in vitro. Therefore, we would like to emphasize here that the in vivo expression of the gene(s) and in vivo binding of the fusion protein to the recognition sites must be definitely investigated once the candidate gene(s) are isolated or identified.

Loss of accessibility of the recognition sequence to the fusion protein can be explained by two possible mechanisms, i.e., chromatin configuration and methylation (Fig. 6). Chromosomal packaging can prevent the access of the transcriptional machinery to nucleosomal DNA, leading to cell-type specific genetic regulation. MMP-1 and -3 expression may be influenced by the chromatin state of the gene, whereby tight chromosomal packaging may interfere with the fusion protein binding. Interestingly, MMP-1 and MMP-3 genes, both of which were not expressed in Ewing sarcoma, have been mapped to the same chromosomal locus, 11q22.3, while the MMP genes which were found to be expressed were mapped to the other loci, implying the possibility that the locus holding MMP-1 and MMP-3 is tightly packaged or silenced. The other possibility is that DNA methylation results in gene inactivation. Methylated DNA-binding proteins are responsible for transcriptional repression via an indirect mechanism, i.e., inhibition of DNA binding of transcriptional factors. Alternatively, DNA binding of ETS transcription factors is sensitive to DNA methylation [45]. Recently, these two mechanisms, i.e., chromatin state and methylation, have been molecularly shown to be tightly linked. Thus, we should be careful before theorizing simply that a putative recognition sequence is essential for the transcription of critical genes, because binding of the fusion protein was shown to be significantly affected in vivo in this study.

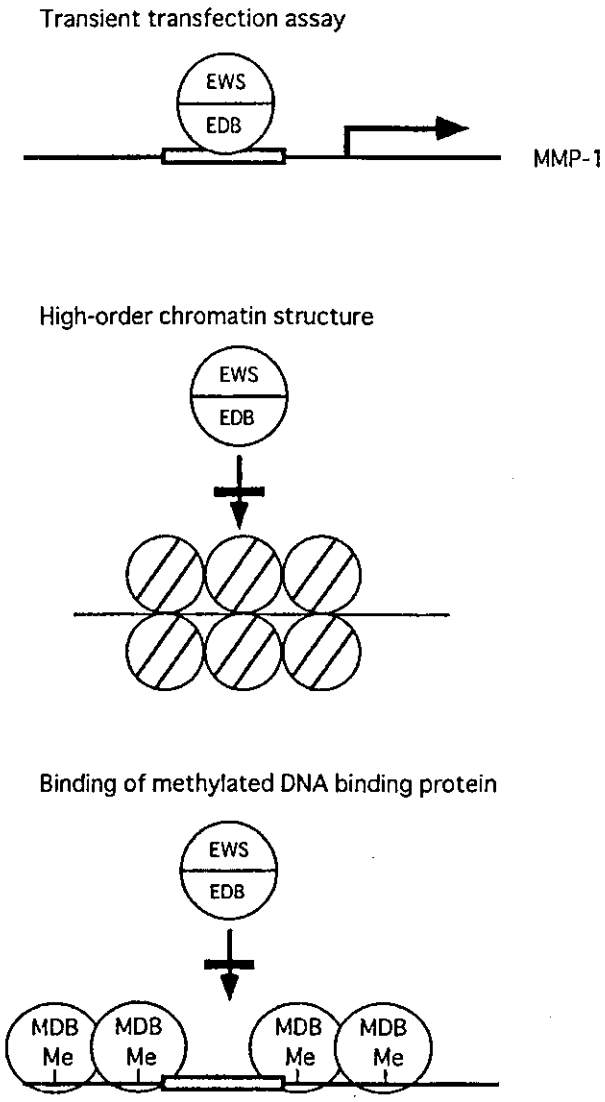

Fig. 6. Loss of accessibility of the MMP regulatory elements to the Ewing sarcoma-specific fusion protein. The chimeric protein between EWS and ETS was found to transactivate the MMPs through binding with the regulatory elements, by a transient transfection assay (A). Two possible mechanisms for this not being the case in vivo are postulated. (B) High-order chromatin structure of the regulatory elements inhibits DNA binding of the fusion protein. (C) Methylated DNA binding proteins prevent the fusion protein from binding to the recognition site.

Acknowledgments

We thank Motoharu Seiki and Hiroshi Sato for their gift of the human MMP-1, -2, -3, -9, MT1-MMP, and TIMP-1, -2 expression vectors. We thank Tadahiro Fujii for his gifts of the cell line (MRC-5) and the MMP-1 (−517/+63)-CAT plasmid, and Hiroo Yabe for his gift of the Ewing sarcoma surgical specimen, KST1420. We thank Akira Hayashi for his gift of the Ewing sarcoma surgical specimen, KST1446. We thank Takatoshi Ohno and Mamoru Ohuchida for their gift of the EWS-FLI-1 and EWS-ERG expression vectors. We also thank Yasunori Okada for his helpful discussion and advice. We dedicate the manuscript to Dr. T. Hirata, our colleague, who died of Ewing/PNET in 1993.

References

[1] J. Ewing, Diffuse endothelioma of bone, Proc. NY Pathol. Soc. 21 (1921) 17–24.
[2] T. Sugimoto, A. Umezawa, J. Hata, Neurogenic potential of Ewing sarcoma cells, Virchows Arch. 430 (1997) 41–46.
[3] A. Crozat, P. Aman, N. Mandahl, D. Ron, Fusion of CHOP to a novel RNA-binding protein in human myxoid liposarcoma, Nature 363 (1993) 640–644.
[4] T.H. Rabbitts, Chromosomal translocations in human cancer, Nature 372 (1994) 143–149.
[5] S. Ishida, K. Yoshida, Y. Kaneko, Y. Tanaka, Y. Sasaki, F. Urano, A. Umezawa, J. Hata, K. Fujinaga, The genomic breakpoint and chimeric transcripts in the EWSR1-ETV4/E1AF gene fusion in Ewing sarcoma, Cytogenet. Cell Genet. 82 (1998) 278–283.
[6] C. Turc-Carel, I. Philip, M. Berger, T. Philip, G. Lemoir, Chromosomal translocations in Ewing sarcoma, N. Engl. J. Med. 309 (1983) 497–498.
[7] J. Whang-Peng, T.J. Triche, T. Knusten, J. Miser, E.C. Douglas, M.A. Israel, Chromosomal translocation in peripheral neuroepithelioma, N. Engl. J. Med. 311 (1984) 584–585.
[8] O. Delattre, J. Zucman, B. Plougastel, C. Desmeze, T. Melot, M. Peter, H. Kovar, I. Joubert, P. de Jong, G. Rouleau, A. Aurias, G. Thomas, Gene fusion with an ETS DNA-binding domain caused by chromosome translocation in human tumors, Nature 359 (1992) 162–165.
[9] J. Zucman, J. Melot, C. Desmaze, J. Ghysdael, B. Plougastel, M. Peter, J.M. Zucker, T.J. Triche, D. Sheer, C. Turc-Carel, P. Ambros, V. Combaret, G. Lenoir, A. Aurias, G. Thomas, O. Dellatre, Combinatorial generation of variable fusion proteins if the Ewing family of tumours, EMBO J. 12 (1993) 4481–4487.
[10] F. Urano, A. Umezawa, W. Hong, H. Kikuchi, J. Hata, A novel chimera gene between EWS and E1A-F, encoding the adenovirus E1A enhancer-binding protein, in extraosseous Ewing sarcoma, Biochem. Biophys. Res. Commun. 219 (1996) 608–612.
[11] P.H. Sorensen, S.L. Lessnick, D. Lopez-Terrada, X.F. Liu, T.J. Triche, C.T. Denny, A second Ewing sarcoma translocation, t(21;22), fuses the EWS gene to another ETS-family transcription factor, ERG, Nat. Genet. 6 (1994) 146–151.
[12] I.-S. Jeon, J.N. Davis, B.S. Braun, J.E. Sublett, M.F. Roussel, C.T. Denny, D.N. Shapiro, A variant Ewing sarcoma translocation (7; 22) fuses the EWS gene to the ETS gene ETV1, Oncogene 10 (1995) 1229–1234.
[13] B.S. Braun, R. Frieden, S.L. Lessnick, W.L. May, C.T. Denny, Identification of target genes for the Ewing sarcoma EWS/FLI fusion protein by representational difference analysis, Mol. Cell Biol. 15 (1995) 4623–4630.
[14] T. Watabe, K. Yoshida, M. Shindoh, M. Kaya, K. Fujikawa, H. Sato, M. Seiki, S. Ishii, K. Fujinaga, The Ets-1 and Ets-2 transcription factors activate the promoters for invasion-associated urokinase and collagenase genes in response to epidermal growth factor, Int. J. Cancer 77 (1998) 128–137.
[15] C. Wasylyk, A. Gutman, R. Nicholson, B. Wasylyk, The c-Ets oncoprotein activates the stromelysin promoter through the same elements as several non-nuclear oncoproteins, EMBO J. 10 (1991) 1127–1134.
[16] G. Buttice, M. Duterque-Coquillaud, J.P. Basuyaux, S. Carrere, M. Kurkinen, D. Stehelin, Erg, an Ets-family member, differentially regulates human collagenase1 (MMP1) and stromelysin1 (MMP3) gene expression by physically interacting with the Fos/Jun complex, Oncogene 13 (1996) 2297–2306.
[17] F. Higashino, K. Yoshida, T. Noumi, M. Seiki, K. Fujinaga, Ets-related protein E1A-F can activate 3 different matrix metalloproteinase gene promorters, Oncogene 10 (1995).
[18] H. Sato, Y. Kida, M. Mai, Y. Endo, T. Sasaki, J. Tanaka, M. Seiki, Expression of genes encoding type IV collagen-degrading metalloproteinases and tissue inhibitors of metalloproteinases in various human tumor cells, Oncogene 7 (1992) 77–83.
[19] A. Kawashima, Y. Okada, I. Nakanishi, Y. Ueda, K. Iwata, A. Roessner, Immunolocalization of matrix metalloproteinases and tissue inhibitors of metalloproteinases in human chondrosarcomas, Gen. Diagn. Pathol. 142 (1997) 129–137.
[20] S. Hara, Y. Adachi, Y. Kaneko, J. Fujimoto, J. Hata, Evidence for heterogenous groups of neuronal differentiation of Ewing sarcoma, Br. J. Cancer 64 (1991) 1025–1030.
[21] C. Homma, Y. Kaneko, K. Sekine, S. Hara, J. Hata, M. Sakurai, Establishment and characterization of a small round cell sarcoma cell line, SCCH-196, with t(11; 22)(q24:;q12), Jpn. J. Cancer Res. 80 (1989) 861–865.
[22] Y. Fujii, T. Hongo, Y. Nakagawa, K. Nasuda, Y. Mizuno, Y. Igarashi, Y. Naito, M. Maeda, Cell culture of small round cell tumor originating in the thoracopulmonary region, Cancer 64 (1989) 43–51.
[23] F. Urano, A. Umezawa, H. Yabe, W. Hong, K. Yoshida, K. Fujinaga, J. Hata, Molecular analysis of Ewing sarcoma: another fusion gene, EWS-E1AF, available for diagnosis, Jpn. J. Cancer Res. 89 (1998) 703–711.
[24] S. Imai, T. Fujino, S. Nishibayashi, T. Manabe, T. Takano, Immortalization-susceptible elements and their binding factors mediate rejuvenation of regulation of the type I collagenase gene in simian virus 40 large T antigen-transformed immortal human fibroblasts, Mol. Cell Biol. 14 (1994) 7182–7194.
[25] A. Umezawa, K. Tachibana, K. Harigaya, S. Kusakari, S. Kato, Y. Watanabe, T. Takano, Colony-stimulating factor 1 expression is down-regulated during the adipocyte differentiation of H-1/A marrow stromal cells and induced by cachectin/tumor necrosis factor, Mol. Cell Biol. 11 (1991) 920–927.
[26] W.A. May, M.L. Gishizky, S.L. Lessnick, L.B. Lunsford, B.C. Lewis, O. Delattre, J. Zucman, G. Thomas, C.T. Denny, Ewing sarcoma 11; 22 translocation produces a chimeric transcription factor that requires the DNA-binding domain encoded by FLI1 for transformation, Proc. Natl. Acad. Sci. USA 90 (1993) 5752–5756.
[27] C.M. Gorman, L.F. Moffat, B.H. Howard, Recombinant genomes which express chloramphenicol acetyltransferase in mammalian cells, Mol. Cell Biol. 2 (1982) 1044–1051.
[28] D.A. Nielsen, J. Chou, A.J. MacKrell, M.J. Casadaban, D.F. Steiner, Expression of a preproinsulin-beta-galactosidase gene fusion in mammalian cells, Proc. Natl. Acad. Sci. USA 80 (1983) 5198–5202.
[29] V. Orlando, R. Paro, Mapping polycomb-repressed domains in the bithorax complex using in vivo formaldehyde cross-linked chromatin, Cell 75 (1993) 1187–1198.
[30] M. Hattori, A. Tugores, L. Veloz, M. Karin, D.A. Brenner, A simplified method for the preparation of transcriptionally active liver nuclear extracts, DNA Cell Biol. 9 (1990) 777–781.